Journal of Digital Imaging

A Computer-aided Multidisease Diagnostic System Using MRCP

Rajasvaran Logeswaran

Automated computer analysis of magnetic resonance cholangiopancreatography (MRCP) (a focused magnetic resonance imaging sequence for the pancreatobiliary region of the abdomen) images for biliary diseases is a difficult problem because of the large inter- and intra-patient variations in the images, varying acquisition settings, and characteristics of the images, defeating most attempts to produce computer-aided diagnosis systems. This paper proposes a system capable of automated preliminary diagnosis of several diseases affecting the bile ducts in the liver, namely, dilation, stones, tumor, and cyst. The system first identifies the biliary ductal structure present in the MRCP images, and then proceeds to determine the presence or absence of the diseases. Tested on a database of 593 clinical images, the system, which uses visual-based features, has shown to be successful in delivering good performance of 70–90% even in the presence of multiple diseases, and may be useful in aiding medical practitioners in routine MRCP examinations.

KEY WORDS: Automated diagnosis, biliary diseases, MRCP, magnetic resonance cholangiopancreatography, liver diseases, structure detection

INTRODUCTION

Magnetic resonance cholangiopancreatography (MRCP)[1,2] is a special sequence of the T1- and T2-weighted magnetic resonance imaging scans, focused on the pancreatobiliary region of the abdomen. This noninvasive nonionizing imaging technique is primarily used to identify diseases and for surgical work-up that affect the biliary system. This system includes the ducts in the liver that produce bile, the gallbladder that stores the bile, and the pancreatic duct. Bile is used in the digestion of fat in the small intestines, and is also used in the removal of wastes (especially fat-soluble ones such as cholesterol) from the body.

Diseases, such as stones in the bile duct, tend to block the ducts, causing a buildup of bile in the ducts, buildup of wastes in the body, and incomplete digestion and absorption of fat-soluble vitamins and minerals. In addition, the biliary ducts dilate, causing a swelling of the liver and can interfere with the performance of the neighboring organs as well. Although routinely used by radiologist to detect diseases, the MRCP images do suffer from several shortcomings, including low resolution, partial volume, large inter- and intrapatient variations in image intensity and orientation, low signal-to-noise ratio, acquisition artifacts, intensity inconsistencies because of object depth and size, and scaling, brightness, and contrast settings. In addition, the quality of the images is also dependent on patient breath-hold, size, and fat and fluid content of the patient's anatomy. It is well known that biological images pose difficulties in automated processing, moreover when the structures in the images vary significantly from patient to patient as in the case of biliary diseases in MRCP images. Although such defects are compensated for by the human visual system and the experience of the specialist during diagnosis, such problems present major difficulties to computer-aided diagnosis (CAD) systems.

This paper proposes a computer-aided system for MRCP, developed to perform automated preliminary diagnosis for several diseases that affect the biliary ducts. The system is able to distinguish healthy images from those with diseases, identifying dilated ducts, stones (cholelithiasis and choledocholithiasis), tumor (cholangiocarcinoma and hepatocellular carcinoma) and choledochol cyst. Tested on clinical MRCP images, the system has shown good performance in detecting the various diseases in 2-dimensional MRCP thick slab and thin slice images.

STRUCTURE IDENTIFICATION

To detect the diseases, the raw MRCP image has to be preprocessed to normalize its characteristics, the biliary structures have to be identified, and the structures are to be analyzed for the various diseases. The general algorithm for the system is given by the flowchart in Figure 1, and described in the following sections.

Image Preprocessing

As large interimage variance is a common phenomenon for MRCP images because of the shape of the structures as well as the acquisition settings that are targeted to obtaining the most suitable images for visual diagnosis, the image
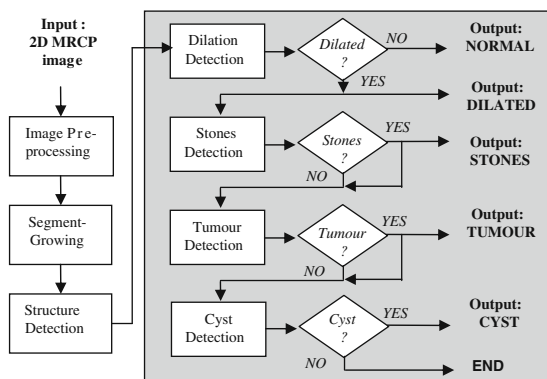

Fig 1. Flowchart of the proposed automated computer-aided multidisease detection system for preliminary diagnosis of four types of biliary diseases using a single 2-dimensional MRCP image.

preprocessing stage is vital in implementing some standardization on the images for the consequent machine-processed stages of the algorithm.

Firstly, images with borders (typical of reprojected 2-dimensional MRCP thick slab images) need to be processed to truncate the borders. This is implemented by removing the zero intensity pixels at the borders of the image, by setting the image to the rectangular area from the top left-most nonzero pixel, until the bottom right-most nonzero pixel. Next, the image is scaled by normalizing its size. This step requires obtaining the image size ratio parameter from the image file header, stored using the digital imaging and communication in medicine[3] standard in the picture archiving and communication system[4] used in the Hospital Information System[5] of medical institutions. The image is scaled using the parameter to restore it to its original size before application of any zooming during acquisition and storage. The third step reduces the influence of air pockets, soft tissues, and noise in the images. Using a histogram-based dynamic filtering technique introduced in Robinson[6] and Robinson and Whelan,[7] the image intensities corresponding to the maximum frequency and below are eliminated. To eliminate bright spots corresponding to artifacts in the image, very high intensities (those beyond two third of the way from the highest significant local maxima on the histogram) are truncated. The middle intensities correspond mainly to the biliary structures. These are stretched so that the truncated histogram covers the image intensity range. As most MRCP images are stored as 12-bpp images, but conventional computer monitors are only capable of 8 bpp, the image intensity range is scaled to be within intensities 0–255.

The mentioned steps produce a more normalized MRCP image for the remaining algorithm. An example of the result of preprocessing an MRCP image is observed in Figure 2, where some of the influences of the background soft tissues, padded border, and fine structures have been removed, and the structures of interest have been enhanced. The removal of artifacts and background is important as it affects structure identification. As such, in addition to the intensity truncation, other features (eg, location) are also used in the "Segment Growing" section to eliminate them as potential seeds.
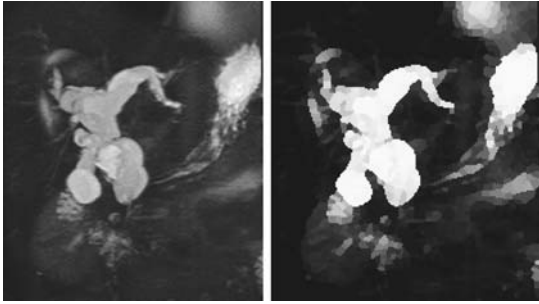
Fig 2. Result (right, normalized image) of preprocessing a 2-dimensional MRCP thick slab reprojected image used in clinical diagnosis (left).

Image Segmentation

The next stage is to identify the possible biliary structures from the resulting image to be able to test these structures for the various diseases. The preprocessed image is split into its components by segmenting it using the watershed algorithm.[8] Watershed is chosen for implementation in this scheme as it is known for good segmentation of MRCP images, as given in Logeswaran[9] and Logeswaran and Eswaran.[10] The goal of the segmentation stage is to treat the image as a cluster of related neighboring pixels rather than treating each pixel individually to overcome pixel level inconsistencies. Once segmented, each pixel is assigned the value of the average intensity of the segment it belongs to, ie, segment intensity averaging, facilitating the treatment of a segment as the unit component for further processing. Each segment is a component of a structure in the image.

The watershed algorithm is also known for its undesired oversegmentation of images. To curb this problem, segment-merging of similar small segments is undertaken, using an adaptation of the technique introduced in Lo et al.[11] Dynamic thresholds are used in the merging, where the combining of segment is undertaken starting with the more significant segments (ie, those with higher intensity) to minimize the possible merging of structure segments with the background. A secondary stop criteria is incorporated to seize merging if the total number of segments are reduced to less than half of its original number to prevent overmerging the segments. The pixels in the newly merged segments are assigned their new corresponding average segment intensity.

Segment Growing

For identification of the biliary structure, a segment-based region-growing approach is undertaken. The preliminary seeds are identified by choosing the high intensity segments. A shortlist of these segments is decided by taking the location of the segments from the image center into account, where because MRCP is a focused imaging technique, the structures of interest (ie, the bile ducts) would be situated close to the center of the image. Conversely, bright segments close to the edges of the image are usually caused by artifacts. The location threshold, or specifically the maximum distance permitted between the segment midpoint and the image center, varies depending on the structure(s) being analyzed. For instance, in the case of choledochal cyst, which would be situated almost at the image center, the distance threshold would be small. However, in the case of tumor, the structures would be further apart (as will be seen later), and thus, a larger threshold is required (although not sensitive to the processing, empirically, values approximately three fourth of the way to the edge of the image were found suitable).

With the selected seeds as the start points, the segments are grown to identify the biliary structures. The criteria for growth are determined through principal component analysis[12] and plotted as graphs. Criteria found suitable in guiding the segment growth (ie, correct and inaccurate results were separable) include average segment *intensity* (structure segments usually have intensities above 200), small *intensity difference* between the two candidate segments to be grown (usually less than 20% of a dynamic value chosen from the 20th percentile of the intensity histogram), *connectivity* of the candidate segments (number of pixels on the shared border, usually 30 pixels or less as large segments are usually part of the background), *distance* between candidate segments (structure segments are small and the midpoints are less than 10 pixels apart), and segment *size* (background segments are usually relatively larger than structure segments which are less than 100 pixels large). Other criteria, such as *direction* of growth, proved to be inconclusive for the growing process. The growing is conducted iteratively, where the first level of segments grown act as seeds for the second level and so
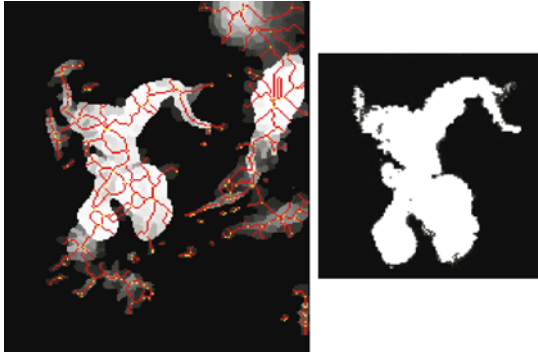
Fig 3. Results of the watershed segmentation (left), thresholded lightly to remove some soft tissue and background segments. The lines indicate the segment boundaries. The segment-grown image (right) shows the detected biliary structure. Some noise, artifacts, and other organs were removed through the structure detection stage.

on. The levels tend to closely correspond to the primary, secondary, and tertiary branches of the biliary tree-like structure, providing additional information that may be derived from the MRCP images. Generally, less than 10 levels are required to identify all the necessary biliary structures.

The segment-growing process was further verified through the manual labeling and growing on 10 clinical MRCP images. The significant biliary structures, mainly the diseased structure for use in this work, were successfully detected in all the test images. Most of the grown segments were also able to identify several levels of the biliary structures in the MRCP images. The segment growing also augments the preprocessing by further removing the influence of noise and non-biliary objects in the image. Figure 3 shows an example of the results achieved by the segmentation and segment-growing stages. The identified biliary structures are used in the disease detection stage.

DISEASE DETECTION

The proposed multidisease system, as given in Figure 1, first differentiates MRCP images containing normal biliary structures from those with diseased structures. The images with diseased structures are generally dilated because of blockages causing bile buildup in the ducts. The

identified structures are examined for each of the diseases in turn. This section describes the features extracted and used in the detection process for each of the diseases.

Dilation

In MRCP images, the normal biliary structures appear as very fine ducts that may sometimes be barely visible. On the other hand, diseased biliary structures are characterized by the abnormal caliber of the biliary structure. The dilation is because of obstructions (eg, tumor) or congenital defects of part or the whole biliary structure, where the ducts are bloated up as the bile is unable to drain out into the lower structures and the small intestines. An example of a normal and a dilated biliary structure are given by the images in Figure 4a, b.

The dilation detection process is given as follows (images that are not detected to contain any dilated structures are considered as normal):

(1) First, each disconnected segment-grown region is labeled individually.
(2) Next, the thickness of the largest region is approximated (by dividing the area of region by the length of its skeleton).
(3) The structure is detected as dilated if:

− Its thickness is greater than 6 pixels (corresponds to 6 mm on the normalized image, which represents the thickness of the largest part of a normal biliary duct), or
− If the area (total number of pixels) of the largest region is greater than 50 pixels (selected experimentally).

Stones

Stones, medically known as choledocholithiasis (stones in the bile ducts) or cholelithiasis (stones in the gallbladder), are essentially smooth, round, calcified structures inside the bile ducts that can hinder the flow of the bile. The algorithm examines dark regions inside the bright biliary structures to detect possible stones, as shown in Figure 4c. The actual intensity of the stone in the MRCP image is dependent on its size, depth within the bile ducts, and acquisition parameter

settings. The segment averaging undertaken in the segmentation stage is useful in noise reduction, but may "hide" some stones.

As such, the algorithm is as follows:

(1) The detected biliary structures are compared with the preprocessed image and the corresponding pixels inside the detected structures are set to the lower of the two intensity values to uncover potential stones.
(2) Next, the intensity of the dark areas inside the detected structures are determined.
(3) The areas with intensity of less 100 (found empirically) are shortlisted as potential stones.
(4) The size (number of pixels) of those dark areas are then determined.
(5) The shortlisted areas of sizes within the range 3–60 pixels (determined empirically) are identified as stones. (Note that the dark areas of less than 3 pixels are inconsistencies in the soft

tissue and those larger than 60 pixels are usually gaps between structures or tumor masses).

Tumor

Tumors affecting the bile ducts are mainly cholangiocarcinoma (tumor of the bile ducts) or secondary obstructions caused by hepatocellular carcinoma (tumor of the liver parenchyma). Tumors can be benign or malignant, irregular shaped, solid masses of mutilated tissue. Although used in the tumor detection and diagnosis, the structures of the tumors are not clearly identifiable in MRCP images as they appear in a variety of intensities (usually in the lower ranges of less than 150 in an 8-bpp image), sizes, and shapes, making detection difficult for computer-aided diagnostic tools. In most cases, the tumor is not a visible

(a) Normal bilairy structure (b) Dilated structure (c) With stones
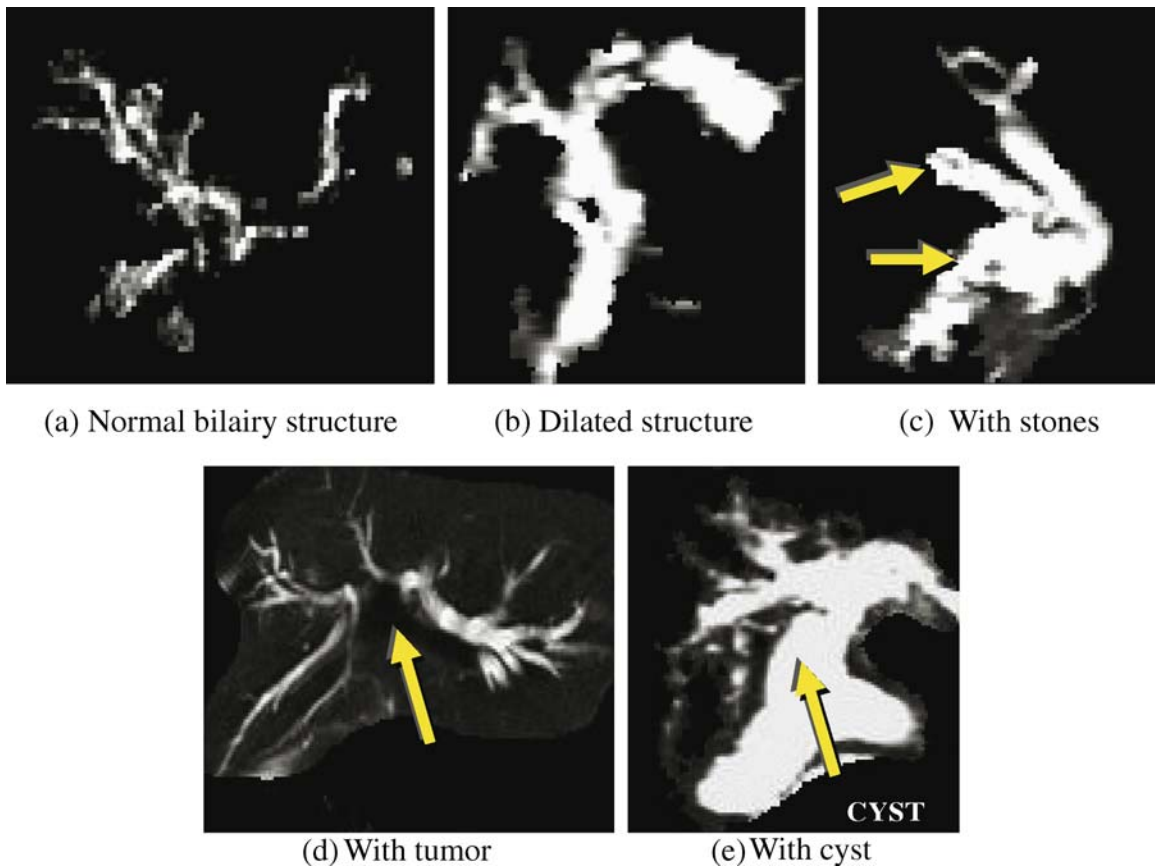
(d) With tumor (e) With cyst

Fig 4. Sample segment-grown biliary structures of 2-dimensional MRCP images denoting the different diseases tested by the system. The shapes and sizes of the biliary structures in MRCP images can vary significantly, thus the images serve only as examples of the main characteristics pertaining to the different diseases.

structure in the T2-weighted 2-dimensional MRCP images, as shown in Figure 4d.

The proposed algorithm is based on the visual interpretation of medical specialists in making their preliminary diagnosis, by analyzing the effect the tumor has on the structure of the biliary ducts. A tumor in the vicinity of the biliary tree in the liver usually causes a partial or complete blockage of parts of the biliary tree structure. This, in turn, causes the biliary ducts to dilate as the bile from the liver is unable to drain into the intestines efficiently. What is observed in the MRCP images would be disconnected dilated biliary ducts. As such, the algorithm (1) identifies the two largest detected biliary structures, (2) determines that both disconnected structures are dilated, and (3) detects tumor if both regions are dilated and located nearby (minimum distance between both structures should be less than 50 pixels as tumors are not too large and a large separation usually indicates independent unconnected structures).

Cyst

Choledochal cysts (cyst inside the bile duct) are usually observed as a fusiform dilation of the central bile duct (CBD). The algorithm (1) checks for larger dilation (detected region size greater than 150 pixels), and (2) detects choledochol cyst if there is dilation in the CBD area (bottom center part of the biliary structure; see Fig. 4e).

PERFORMANCE EVALUATION

The performance achieved by the proposed system on a clinical database of 593 2-dimensional MRCP images is given in Table 1 in terms of the popular true positive (*TP*, number of correctly detected diseased cases), true negative (*TN*, number of correctly identified nondiseased cases), *sensitivity* (also known as the TP rate), *specificity* (also known as the TN rate), as well as the *overall* performance measures. The sensitivity and specificity pair gives the likelihood of the test successfully identifying the tested feature.[13] This statistical pair is widely used for the evaluation of many software systems, and gives a good gauge of the performance of an algorithm. As the test set used contains images for a number of diseases, the *overall* performance of an algorithm in detecting the presence and absence of a disease out of the entire test set is also given. The statistics used are calculated as follows, where *FN* is the false negative (number of positive cases detected as negative) and *FP* is the false positives (number of negative cases detected as positive):

$$\text{Sensitivity} = TP/(TP + FN) \qquad (1)$$

$$\text{Specificity} = TN/(TN + FP) \qquad (2)$$

$$\text{Overall} = (TP + TN)/(TP + TN + FP + FN) \qquad (3)$$

The results presented in Table 1 are that of the performance achieved through several iterations of testing by experimentally selecting parameter values to maximize the overall results. The results for sensitivity, specificity, and overall are reported as percentages (cf. ratios). Generally, it is found that the proposed system is able to effectively conduct automatic preliminary diag-

Table 1. Performance Achieved by the Proposed Multidisease Preliminary Diagnosis System for Biliary Diseases

	Dilation	Stone	Tumor	Cyst
TP	327	71	33	8
TN	129	354	478	523
Sensitivity (%)	94.78	53.80	54.10	25.00
Specificity (%)	52.02	76.80	89.85	93.23
Overall (%)	76.90	71.67	86.17	89.55

Testing is conducted on a test set of 593 clinical 2-dimensional MRCP images, containing 248 images with normal biliary structures and 345 images with dilated biliary structures (132 with stones, 61 with tumor, 32 with cyst, and the remaining 120 with dilation because of other causes, eg, residual postsurgery dilation, Klatskin's disease, Caroli's disease, strictures, and obstruction from other liver diseases).

nosis for multiple biliary diseases, using quick, simple, visually oriented features. The system achieved more than 70% detection rate for all the tested diseases on 2-dimensional MRCP images.

It is possible to improve the other statistics, compromising the overall result. Such adjustments should be undertaken based on the priority and significance of the results. For instance, if it is deemed that a conservative practice of FP would be more prudent, so that minimum positive cases are overlooked and that overtesting is better than undertesting (eg, for deadly diseases), the parameter values or thresholds may be reduced. On the other hand, if the disease is not serious (especially at the early stages, where it is less prominent and thus not detected by the algorithm), and testing cost and patient discomfort is more of a priority, lower sensitivity may be preferred and the thresholds may be increased.

There are some limitations to the proposed system. The system is susceptible to poorly oriented images, and those with low resolution, as the visibility of the biliary structures are hampered in such images. However, such images pose a problem during the clinical visual diagnosis as well and radiologists are usually not willing to make a diagnosis with such images (ie, very poor quality images are discarded from the image series acquired for the examination during diagnosis). In the case the intensity of the background tissue being uncharacteristically high, the structure detection may not be able to distinguish the boundaries of the ducts from the soft tissue and may wrongly detect some of the background as part of the biliary structures. This could cause air pockets and folds in the images to be misdiagnosed as stones. For the detection of choledochol cyst, the standardization of orientation and focus of the acquisition has to be maintained to correctly identify the CBD. Otherwise, other structures, mainly the gallbladder, may appear as a dilated CBD. Most of the limitations of the system are overcome through proper standardization of the acquisition series and parameter settings.

CONCLUSION

Magnetic resonance cholangiopancreatography images are difficult to process automatically because of the complexities involved in the biliary structure shapes, intensities, orientations, acquisition settings, breathing artifacts, noise, background soft tissue, overlap of other organs, etc. Furthermore, even established medical practitioners utilize series of MRCP images, visual experience, and anatomical knowledge to conduct diagnosis. This paper tackles the problem by proposing a computer-aided solution that extracts the biliary structure information from 2-dimensional MRCP images, and utilizes visually based features to provide preliminary diagnosis of several biliary diseases by analyzing individual MRCP images (instead of the entire series). As existing clinical images used for actual diagnosis in the collaborating hospital was used in this research (as opposed to images specifically catered for this research), several thresholds had to be selected experimentally to cater for the wide variety of settings and parameters, as well as operator experience over several years of image acquisition. The values mentioned in this paper were found to be suitable for a large number of images, and subject to visual comparison with recorded diagnosis, as well as in consultation with the senior radiologist.

Performance tests on a clinical database of 593 MRCP images from the collaborating medical institution shows that the proposed system was able to achieve more than 70% correct diagnosis of each disease. This encouraging results allows such automated systems to aid medical practitioners in quick preliminary diagnosis or large numbers of images, typical of complete MRCP examinations. It is also hoped that the proposed system paves the way for more CAD systems for MRCP and biliary diseases of the liver.

ACKNOWLEDGMENTS

REFERENCES

1. Ernst O, Calvo M, Sergent G, Mizrahi D, Carpentier F: Breath-hold cholangiopancreatography using a HASTE sequence: comparison of single-slice and multislice acquisition technique. AJR Am J Roentgenol 169:1304–1306, 1997

2. Justus A, Govil S, Korah I: Non-breath-hold magnetic resonance cholangiography—preliminary results and review of literature. Indian J Radiol Imaging 9(2):53–58, 1999

3. ACR/NEMA: Standards Publication PS3/DICOM 3 (Digital Imaging and Communications in Medicine Standard). ACR/NEMA, 1993

4. BSHSI/TEWS: White Paper—Picture Archiving and Communications Systems. BSHSI/TEWS, 2004. Available at http://www.bshsi.com/tews/docs/TEWS.PACS%20Overview.pdf

5. Kurihara Y, Okuhara Y, Narita Y, Kitazoe Y, Sawada A, Yoshida S: Integration of medical images into the total Hospital Information System—experiences at Kochi Medical School. In: Proceedings of the 32nd Annual Hawaii International Conference on System Science, volume 4, 1999, pp 1–8

6. Robinson K: Efficient pre-segmentation filtering in MRCP. Ph.D. thesis, Ireland: Dublin City University, 2005

7. Robinson K, Whelan PF: Analysis of the pancreato-biliary system from MRCP. In: Proceedings of the 18th IEEE International Symposium on Computer-based Medical System (CBMS), Dublin, Ireland, 2005, pp 253–258

8. Olsen Multi-scale watershed segmentation. Gaussian Scale Space Theory, Kluwer Academic Publishers, 1997, pp 191–200

9. Logeswaran R: Scale-space segment growing for hierarchical detection of biliary tree structure. Int J Wavelets Multiresolut Inf Process 3(1):125–140, 2005

10. Logeswaran R, Eswaran C: Application of 3D multiresolution analysis for structure detection in 2D. Multimed Cyberscape J 3(4):30–34, 2005

11. Lo P, Bister M, Eswaran C: Watershed segmentation with gradient threshold and root merging for ultrasound images. In: Proceedings of the South-East Asian Congress of Medical Physics (SEACOMP) and Asian-Oceania Congress of Medical Physics (AOCMP), Kuala Lumpur, Malaysia, 2004, pp 251–256

12. Gonzalez RC, Woods RE: Digital Image Processing, 2nd edition. NJ: Prentice Hall, 2002

13. Synder J: What is a false positive. Network World, 2004. Available at http://www.networkworld.com/reviews/2004/122004spamside3.html